

Structural Transition of Wigner Crystal on Liquid Substrate

M. Haque,* I. Paul,† and S. Pankov

Physics Department, Rutgers University, New Jersey, USA

(Dated: November 19, 2018)

The physics of an electron solid, held on a cryogenic liquid surface by a pressing electric field, is examined in a low-density regime that has not been explored before. We consider the effect of the pressing field in distorting the surface at the position of each electron and hence inducing an attractive force between the electrons. The system behavior is described in terms of an interplay between the repulsive Coulomb interaction and the attractive surface-induced interaction between individual electrons. For small densities and large enough pressing fields, we find a parameter regime where a square lattice is more favorable than the usual triangular lattice; we map out the first-order transition curve separating the two lattice geometries at zero temperature. In addition, our description allows an alternate static perspective on the charge-density wave instability of the system, corresponding to the formation of multi-electron dimples.

I. INTRODUCTION

The crystallization of charged particles due to Coulomb repulsion, first predicted by Wigner¹, has been under discussion in the context of 2D electron systems on cryogenic substrates²⁻⁵ and in semiconductor heterojunctions¹⁴. Wigner crystallization has also been studied in three-dimensional trapped-ion systems¹⁵. The situation in semiconductor junctions, unfortunately, has been obscured by the presence of disorder¹⁴. Electrons held on a liquid helium surface by a pressing electric field, on the other hand, provided the first clean realization of a Wigner crystal^{3,4}.

For the case of electrons on a cryogenic liquid substrate, the presence of a distortion-prone surface introduces additional physics. In this paper we investigate a previously-unexplored effect of the surface on the electron crystal, in a low-density regime that has not yet been probed experimentally.

Experiments with two-dimensional electron systems on liquid helium are done with a pressing field E_{\perp} that holds the electrons to the liquid surface. One effect of the pressing field, that has been studied in depth by a number of authors⁵⁻⁸, concerns a regime of density high enough so that one can treat the surface as a uniformly charged sheet. In this regime of large electron density n , as one increases E_{\perp} to a certain value, the surface breaks up into many-electron dimples, the size of the dimples being given by the capillary length of the liquid. The dimples themselves form a triangular lattice⁵⁻⁸. This situation describes a significant part of the E_{\perp} - n phase diagram.

At smaller densities, it seems sensible to consider the effect of the pressing field on individual electrons: each electron forms a single-electron dimple. (Since the physics determining the shape of these dimples is the same as that for multi-electron dimples, they have the same shape, on different scales.) Single-electron dimples have been studied previously, especially in the context of forming a self-trapped polaronic state⁹. However, the formation of such dimples for each electron should also cause a 'mattress-effect' attraction between any two electrons, and to the best of our knowledge the effects of this surface-induced interaction have not been explored.

The surface-mediated attractive interaction between electrons introduces new physics in the 2D system. One possibility is one or more structural phase transitions. Our analysis shows that, in a low- n , high- E_{\perp} segment of the E_{\perp} - n phase diagram, a square lattice is energetically more favorable than the usual triangular lattice. We thus prove the existence of at least one structural transition. In addition, some of the traditionally-known surface effects, such as the surface-buckling instability, can be interpreted from a fresh perspective using the idea of competition between attractive and repulsive interactions.

Two-dimensional electrons have been studied on several cryogenic systems², e.g., surfaces of liquid ⁴He and liquid ³He, at ⁴He-³He interfaces, the interface between solid and superfluid ⁴He, etc. In recent times, experimental efforts have concentrated on increasing electron densities, and on using thin liquid films, for example for the purpose of observing a solid-to-liquid quantum phase transition in the low-temperature, high-density direction^{12,13}. Other experiments include investigations of the effects of a magnetic field on excitation and transport properties, and the study and control of de-coherence¹⁹ for quantum-computing purposes.

In section II we derive the form of the attractive interaction between two electrons due to surface deformations caused by the pressing field pushing the electrons down. In section III we discuss general properties of systems formed by a combination of attractive and repulsive forces, and outline the consequences for the system we are describing. The energy calculations for the relative stability of square and triangular lattices are outlined in section IV, and section V describes details of the numerics and the resulting phase-diagram.

II. SURFACE-INDUCED INTERACTION

We consider a system of N electrons, held at positions \mathbf{r}_i on the surface of a thick cryogenic (possibly helium) liquid substrate by a pressing electric field of magnitude E_\perp perpendicular to the surface. We will calculate the surface-mediated interaction from classical, static considerations.

We will use $u(\mathbf{r})$ to denote the vertical displacement of the surface at point \mathbf{r} , as compared to the undistorted (flat) configuration. We proceed to write down the energy as a functional of $u(\mathbf{r})$. There are three contributions: a surface tension term describing the energy cost due to surface distortion, a pressing-field term describing the energy that the electron gains due to vertical displacement, and a gravity term describing the bulk displacement of helium accompanying the surface distortion.

$$E[u(\mathbf{r})] = \sigma \int d^2r \left[1 + (\nabla u(\mathbf{r}))^2 \right]^{1/2} + eE_\perp \sum_{i=1}^N u(\mathbf{r}_i) + \frac{g\rho}{2} \int d^2r [u(\mathbf{r})]^2 .$$

Here σ and ρ are respectively the surface tension and density of helium. The pressing electric field E_\perp actually contains contributions from both the externally applied field and the field due to the image charge formed by the helium dielectric. We will be interested in large applied fields, compared to which the dielectric effect is negligible.

Expanding the surface-tension term to lowest order in ∇u , we get in momentum space:

$$E[u(\mathbf{k})]_{\{\mathbf{r}_1, \dots, \mathbf{r}_N\}} = \frac{A\sigma}{2} \sum_{\mathbf{k}} k^2 u(\mathbf{k}) u(-\mathbf{k}) + eE_\perp \sum_{i=1}^N \sum_{\mathbf{k}} u(\mathbf{k}) e^{i\mathbf{k}\cdot\mathbf{r}_i} + \frac{Ag\rho}{2} \sum_{\mathbf{k}} u(\mathbf{k}) u(-\mathbf{k}) .$$

The \mathbf{k} are 2D wave-vectors and A is the area; $4\pi^2 \sum_{\mathbf{k}} \leftrightarrow A \int d^2k$. The form of $u(\mathbf{k})$ is now determined by minimizing the energy functional. The result is

$$u(\mathbf{k}) = - \frac{eE_\perp}{A\sigma} \sum_{i=1}^N \frac{e^{-i\mathbf{k}\cdot\mathbf{r}_i}}{k^2 + l_0^{-2}} = \sum_{i=1}^N u_1^{\mathbf{r}_i}(\mathbf{k}) . \quad (1)$$

Here $l_0 = \sqrt{\sigma/g\rho}$ is the capillary length of the liquid substrate; it will be the important length scale in all our considerations. Also,

$$u_1^{\mathbf{r}_i}(\mathbf{k}) = - \frac{eE_\perp}{A\sigma} \frac{e^{-i\mathbf{k}\cdot\mathbf{r}_i}}{k^2 + l_0^{-2}}$$

is the Fourier transform of the distortion due to a *single* electron at \mathbf{r}_i , i.e., the shape of a single-electron dimple, as can be easily verified by minimizing the energy functional for a single-electron system.

The energy of the system is the minimum of the functional $E[u(\mathbf{k})]$, and can be now written in terms of the $u_1^{\mathbf{r}_i}$'s:

$$E(\mathbf{r}_1, \dots, \mathbf{r}_N) = \frac{A\sigma}{2} \sum_{\mathbf{k}} (k^2 + l_0^{-2}) \sum_{i=1}^N u_1^{\mathbf{r}_i}(\mathbf{k}) \sum_{j=1}^N u_1^{\mathbf{r}_j}(-\mathbf{k}) + eE_\perp \sum_{i,j} \sum_{\mathbf{k}} u_1^{\mathbf{r}_i} e^{i\mathbf{k}\cdot\mathbf{r}_j},$$

which separates into diagonal ($i = j$) and non-diagonal ($i \neq j$) pieces:

$$E(\mathbf{r}_1, \dots, \mathbf{r}_N) = NE^{(1)} + \sum_{i < j} V(\mathbf{r}_i - \mathbf{r}_j), \quad (2)$$

with

$$E^{(1)} = - \frac{(eE_\perp)^2}{2A\sigma} \sum_{\mathbf{k}} (k^2 + l_0^{-2})^{-1}, \quad V(\mathbf{r}_i - \mathbf{r}_j) = - \frac{(eE_\perp)^2}{A\sigma} \sum_{\mathbf{k}} \frac{e^{i\mathbf{k}\cdot(\mathbf{r}_j - \mathbf{r}_i)}}{k^2 + l_0^{-2}}$$

The first term of eq (2) is an extensive quantity representing the energy of N independent electrons. The second term gives the attractive interaction energy between the electrons mediated by surface deformation. We have thus obtained the 'mattress'-effect attractive potential to be

$$V(\mathbf{r}) = - \frac{(eE_\perp)^2}{4\pi^2\sigma} \int d^2k \frac{\cos(\mathbf{k}\cdot\mathbf{r})}{k^2 + 1/l_0^2} = - \frac{(eE_\perp)^2}{2\pi\sigma} K_0(r/l_0). \quad (3)$$

Here K_0 is the zeroth-order Bessel function of the second type. It has the asymptotic behavior $K_0(x) \sim -\log(x)$ for $x \rightarrow 0$ and $K_0(x) \sim (\pi/2x)^{1/2}e^{-x}$ for $x \rightarrow \infty$.

Two comments are in order concerning this derivation. First, the electrons have been treated as point objects, and this leads to interactions and dimple shapes that diverge logarithmically at small distances. This divergence is cured by the fact that the electron wavefunction has a finite spatial width. In this work we will not attempt a calculation of this wavefunction width, but will assume that this spatial extension is much smaller than the lattice spacings which we consider. This assumption is particularly reasonable in the low-density region, deep in the solid phase, that we focus on.

Second, we have retained only the $(\nabla u)^2$ term in the surface-tension energy. This is equivalent to keeping only the pairwise interaction between electrons and dropping four-electron and higher terms. For quantitative calculations, eq (3) is used only in a very-low-density regime; effects of four-body or higher terms are expected to be small here. Our order-of-magnitude estimates in section III concerning moderate-to-high densities makes use only of qualitative ideas from the mattress-effect calculation, because in this regime the effect of higher-order terms is expected to be important.

III. EFFECTS OF ATTRACTIVE INTERACTION: GENERAL REMARKS

The Wigner lattice on a helium substrate is formed by electrons which interact via a Coulomb repulsion and a surface-mediated attraction:

$$V(\mathbf{r}) = V_{\text{coul}}(\mathbf{r}) + V_{\text{surf}}(\mathbf{r}) = \frac{e^2}{r} - \frac{(eE_{\perp})^2}{2\pi\sigma}K_0(r/l_0). \quad (4)$$

The effect of the surface term has not been considered in detail before, and we shall proceed to do so in the present paper.

The surface-induced attraction can be tuned by controlling the pressing electric field E_{\perp} . At short enough distances, the $1/r$ function dominates over the logarithmic surface term, and at large r the Coulomb term again dominates over the exponentially decreasing attraction. V_{surf} can compete with V_{coul} only at intermediate distances. As E_{\perp} is ramped up, the distance scale at which V_{surf} first becomes comparable to V_{coul} is $r \sim l_0$.

In general, when microscopic objects interact via attractive and repulsive potentials of different ranges, several things can happen depending on the relative strengths and ranges of the attractive and repulsive forces. First, consider the case of repulsive forces alone, or short-range repulsion coupled with longer range attraction. This situation tends to create microscopic-ordered phases, such as Wigner crystals, vortex lattices and skyrmion lattices¹⁶. Second, when the attractive force dominates at all distances, the system tends to collapse. One example is what happens at the higher critical magnetic field H_{c2} of a Type-II superconductor: the interaction between vortices of the mixed phase becomes attractive at $H = H_{c2}$, and this leads to collapse of the vortex matter so that the system is filled with the normal electrons of the vortex cores, and superconductivity is destroyed. And finally, a combination of short-range attraction and long-distance repulsion tends to create intermediate-scale order, or ‘‘clustering’’. Examples are charge density waves in solids and quantum hall systems.

This approach enables us to view the well-known electrohydrodynamic (surface-buckling) instability of this system⁵⁻⁸ from a novel perspective. For an electron density much larger than l_0^{-2} , any electron has a large number of electrons within a distance less than the capillary length l_0 from itself, so that the attractive force due to surface distortion acts between a large number of particles. Thus we have an attractive interaction at intermediate distances and a long-distance Coulomb repulsion. Therefore when the attractive interaction is ramped up by increasing the electric field, one can expect from the preceding general discussion the formation of intermediate-scale clusters, which are themselves ordered in a regular pattern.

This is exactly the phenomenon of formation of many-electron dimples that is observed for high-density electrons under large pressing fields. Previously this instability has been studied in terms of the excitation spectrum of a surface approximated as being uniformly charged⁵⁻⁸. In the traditional analysis, one finds that at a certain pressing field, the spectrum goes ‘‘soft’’ at wavenumber $k \sim l_0^{-1}$, indicating the onset of a charge-density instability of this wavenumber. The pressing field at which this spectrum softening first happens is given by $E_{\perp}^2 = 4\pi[\rho g\sigma]^{1/2} - (2\pi ne)^2$, or $E_{\perp} \approx [16\pi^2\rho g\sigma]^{1/4}$ at low densities.

In our picture of competition between attractive and repulsive forces, the formation of multi-electron dimples (intermediate-scale order) would occur when the attractive term V_{surf} starts to dominate over the repulsive term at intermediate or small distances. This viewpoint allows a simple calculation of the pressing field at which the surface-buckling occurs: it is the pressing field for which we have $V_{\text{surf}}(r = l_0) \approx V_{\text{coul}}(r = l_0)$, i.e., $E_{\perp} \approx \{[K_0(1)]^{-2} 4\pi^2\rho g\sigma\}^{1/4} \approx 1.1 [16\pi^2\rho g\sigma]^{1/4}$, within 10% of the traditional result.

Next we want to concentrate on a lower-density regime, $n \gtrsim 1/l_0^2$, where we find a less dramatic but nevertheless important effect of the competition between attractive and repulsive forces. As the inter-particle distance approaches l_0 , the formation of many-particle dimple becomes less likely, since there is no longer “many” electrons within the capillary-length scale, and the uniform-smear charge approximation becomes untenable. It is not clear whether a surface-buckling instability is still present. However, one still expects some effects of increasing attraction as E_\perp is ramped up. One possibility is a structural transition to a different lattice geometry. In the remainder of the paper, we show that there is indeed a region of E_\perp - n space where a square lattice becomes more favorable to the triangular lattice for the Wigner crystal.

Bonsall and Maradudin’s classic work¹⁰ (referred to as BM from now on) has shown for a 2D electron lattice, where the electrons interact via a Coulomb force only, that the triangular (hexagonal) lattice is energetically the most stable of all five Bravais lattices. This is simple to understand physically, because for different 2D lattices corresponding to the same density, the triangular lattice is the one with largest lattice spacing; the electrons thus minimize the repulsive energy by staying as far away as possible from each other. Presumably, the triangular lattice is also the most stable for purely repulsive potentials of other forms, because the same argument holds. However, when one adds an attractive force, one of the other lattice shapes may become more favorable. For example, the lattice spacing is a factor of $(2/\sqrt{3})^{1/2}$ smaller for a square lattice of the same density, and so the attractive energy can possibly be lowered by choosing this lattice geometry. Of course the number of nearest neighbors is also smaller for the square lattice, so which lattice geometry is energetically favorable depends on the exact forms and relative strengths of the attractive and repulsive interactions.

IV. TRIANGULAR VS SQUARE LATTICE

At finite temperature, the lattice geometry that is more favorable is the one with lower free energy $F = E - TS$. We will restrict ourselves to zero temperature, so that it is sufficient to consider the energy E of the two lattices.

Using the two-electron potential (eq 4), one can simply sum up all pairwise interaction energies for the square lattice and the triangular lattice, and then compare. Instead, we will look at a slightly different quantity, as in BM¹⁰. We will consider the electron located at the origin and let E denote the energy of the interaction of this electron with all the other electrons. The total energy of the lattice of N electrons is then $\frac{1}{2}NE$. We compare triangular and square lattices:

$$E^{\text{TR}} = \sum_{\mathbf{R}_i \neq 0} V(\mathbf{R}_i^{\text{TR}}), \quad E^{\text{SQ}} = \sum_{\mathbf{R}_i \neq 0} V(\mathbf{R}_i^{\text{SQ}})$$

Here $\mathbf{R}_i^{\text{TR(SQ)}}$ runs over the positions of all the electron positions in the triangular (square) lattice, and $V(\mathbf{r})$ is the potential (eq. 4) consisting of a Coulomb repulsion and a surface-mediated attraction. The two lattices each have the same density n .

We will look at the difference,

$$\Delta E = E^{\text{TR}} - E^{\text{SQ}} = \Delta E_{\text{coul}} + \Delta E_{\text{surf}}, \quad (5)$$

between the triangular and square lattices. The square lattice is more stable if ΔE is positive. The Coulomb part,

$$\Delta E_{\text{coul}} = \sum_{\mathbf{R}_i \neq 0}^{(\text{TR})} \frac{e^2}{\mathbf{R}_i^{\text{TR}}} - \sum_{\mathbf{R}_i \neq 0}^{(\text{SQ})} \frac{e^2}{\mathbf{R}_i^{\text{SQ}}}, \quad (6)$$

is known to be negative, since the triangular lattice is the most stable under Coulomb forces alone, and has been studied in detail in BM¹⁰. In terms of density, their results are

$$\Delta E_{\text{coul}} = (-3.921034)e^2 n^{1/2} - (-3.900265)e^2 n^{1/2} = -(0.020769)e^2 n^{1/2}$$

As for the surface part,

$$\Delta E_{\text{surf}} = \frac{e^2 E_\perp^2}{2\pi\sigma} \left\{ - \sum_{\mathbf{R}_i \neq 0}^{(\text{TR})} K_0(|\mathbf{R}_i^{\text{TR}}|/l_0) + \sum_{\mathbf{R}_i \neq 0}^{(\text{SQ})} K_0(|\mathbf{R}_i^{\text{SQ}}|/l_0) \right\} = \frac{e^2 E_\perp^2}{2\pi\sigma} S_{\text{surf}}, \quad (7)$$

it is not *a priori* obvious that this is positive, but numerical calculations confirm that it is. The transition corresponds to the values of E_\perp and n for which the two terms just cancel each other out, $\Delta E_{\text{surf}} = -\Delta E_{\text{coul}}$, i.e.,

$$E_\perp^{\text{transition}} = \sqrt{(2\pi\sigma)(0.020769)(2/\sqrt{3})^{1/2} n^{1/2} (S_{\text{surf}})^{-1}}. \quad (8)$$

Zero-Temperature Phase Diagram

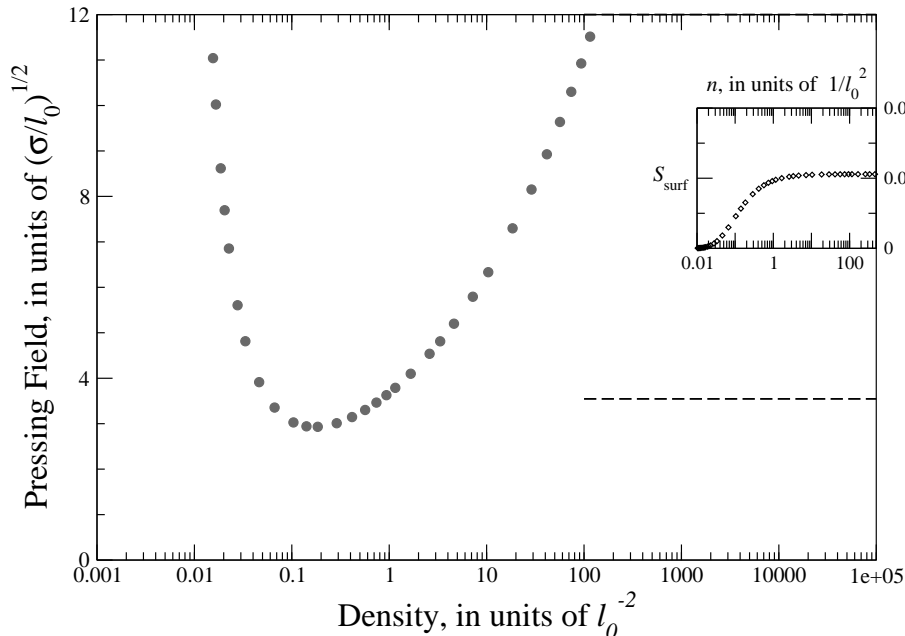


FIG. 1: E_{\perp} vs n phase diagram. Large dots, from numeric computation, map out the line where triangular and square lattices have the same energy. In the region above this curve, the square lattice is more favorable. The horizontal line indicates the spectrum instability, corresponding roughly to the transition to the surface-buckled, multi-electron dimple state. At higher densities this curve should move downward (eq 9); this density-dependence is not shown here. The inset shows the quantity S_{surf} (eq 7), determined numerically, reaching a constant value at densities $\gg l_0^{-2}$.

To map out the transition line exactly, we need to numerically calculate S_{surf} ; the numerical results are shown in figure 1.

We can also analytically predict the dependence of S_{surf} and E_{\perp} on the density for larger densities ($n \gg l_0^{-2}$). The approximation $K_0(r/l_0) \approx -\ln(r/l_0)\theta(l_0 - r)$ is good for $r \ll l_0$. Using this “logarithmic” approximation, we argue in appendix A that S_{surf} becomes independent of n , at large n . Therefore from eq (8) one finds the shape $E_{\perp} \sim \sqrt{\sigma}n^{1/4}$ for the transition curve in the E_{\perp} - n plane, for densities much larger than $l_0^{-2} = \rho g/\sigma$.

Since the surface-mediated attraction falls off quickly for increasing inter-electron distances, one would need stronger electric fields at lower densities to have comparable attractive and repulsive interactions. Therefore the transition curve should rise steeply on the lower- n side, for $n < l_0^{-2}$. In the logarithmic approximation the left (lower- n) side of the transition curve is simply a vertical line at $n = l_0^{-2}$.

V. ZERO-TEMPERATURE PHASE DIAGRAM

The zero-temperature phase diagram in the E_{\perp} -density plane is shown in figure 1. E_{\perp} and n are plotted in units of $\sqrt{\sigma/l_0}$ and $1/l_0^2$ respectively; this guarantees that the same phase diagram is applicable to different cryogenic substrates, one simply has to replace the numerical values of σ and $l_0 = \sqrt{\sigma/g\rho}$ for the particular liquid being used.

The transition line $E_{\perp}(n)$ is found by calculating $S_{\text{surf}} = -\sum^{\text{TR}} K_0(r_i) + \sum^{\text{SQ}} K_0(r_i)$ numerically and then using eq (8). BM, in doing the corresponding sum for the Coulomb potential¹⁰, use an Ewald sum to convert the summation over $1/r$ to a summation over a faster-decaying function. Since K_0 is rapidly-decaying itself, no such procedure is necessary for our case. Also, BM use a renormalization procedure (subtracting off contribution due to spread-out positive charge) to get a finite energy for each lattice geometry. This is again unnecessary because the sums converge for the short-ranged K_0 function.

Our analytical calculation of the high-density side of the phase-transition line is actually very good; a $E_{\perp} \sim n^{1/4}$ fit matches the numeric curve quite spectacularly. On the lower- n side, the minimum of the curve is at about an order-of-magnitude lower than l_0^{-2} . The rise of the curve at small density is not quite as dramatic as the vertical line predicted by the logarithmic approximation.

At higher densities, there is an E_{\perp} above which the electrons cluster into multi-electron dimples (which themselves form a triangular lattice). As far as we know, a detailed calculation of the exact transition line between the single-electron Wigner crystal state and the surface-buckled multi-electron dimple lattice has never been performed, but a simple estimate is obtained by considering the instability in the spectrum of a uniformly charged liquid surface⁸:

$$E_{\perp} = \sqrt{4\pi[\rho g \sigma]^{1/2} - (2\pi n e)^2}. \quad (9)$$

The low-density part of this curve is the horizontal line in the phase diagram, figure 1. The n -dependent deviation due to the $(2\pi n e)^2$ term is substrate-dependent, even with our choice of units for E_{\perp} and n , and is important only at very high densities, and so is omitted from the plot.

VI. CONCLUDING REMARKS

In summary, we have reported a novel effect of surface distortions on the Wigner crystal formed by electrons deposited on a liquid substrate. Our analysis shows that, at low electron densities, there is a significant portion of the zero-temperature E_{\perp} - n phase diagram where a square lattice is energetically more favorable than the usual triangular lattice. Since we have not done a stability analysis of the square lattice under the combined interaction of eq (4), we cannot yet say whether the square lattice is stable, or whether some lattice geometry other than square and triangular is the actual stable geometry. However, the energy calculation proves quite clearly the presence of at least one structural phase transition at low densities.

The structural transition in this system is particularly remarkable because it arises from the interplay of two very simple forces, a long-range repulsion and a short-range attraction. Other physical systems for which structural transitions have been discussed (crystalline solids¹⁸, flux-line lattices, skyrmion lattices^{16,17}) tend to involve far more complicated interactions between the constituents.

Experiments on this system have, until now, probed only densities significantly larger than l_0^{-2} . For ⁴He, the capillary length corresponds to $l_0^{-2} \approx 400 \text{ cm}^{-2}$, while typical experimental Wigner-crystal densities are in the range $\sim 10^5$ - 10^9 cm^{-2} . The same situation holds for explored electron densities on other surfaces and interfaces. To the best of our knowledge, there have been no experimental efforts aimed at exploring the electron crystal structure at very low densities ($n \sim l_0^{-2}$). One possible experimental signature of a structural transition to a different geometry would be a shift in the resonance positions in a Grimes-Adams⁴ type experiment.

The analysis in the present work, in addition to the prediction of at least one structural transition, poses several questions. First, there is the issue of the region of parameter space in which the triangular and square lattices are actually stable. Stability questions can be investigated by studying the dynamical matrix or the elastic constants¹⁸. Instability of both lattices in some part of the E_{\perp} - n plane would indicate that a different geometry is more favorable than both the lattices we have considered. (Situations in which more than two lattice types are important have been encountered previously in the context of skyrmion lattices¹⁷.) In such a case there is the added question of what lattice, or other structure, is the actual stable one. One way to find out is to calculate the lattice energies for all five Bravais lattices (as done for the pure coulomb case in BM¹⁰), or better yet, for all possible lattice geometries, parameterized in a suitable way. And finally, there is the question of crossover between single-electron lattice structures to many-particle dimple lattice structures as one increases the electron density at high E_{\perp} . One immediately plausible speculation is that this transition may proceed via a dimerization. Several of these issues are the subject of ongoing calculations and will appear in a future publication.

Acknowledgments

We thank I. Skachko, R. Chitra, E.Y. Andrei, B.I. Halperin and M.H. Cohen for useful discussions.

APPENDIX A: DEPENDENCE OF S_{surf} ON DENSITY

For densities significantly larger than $n_0 = 1/l_0^2$, we use $K_0(r/l_0) \approx -\ln(r/l_0)\theta(l_0 - r)$ and get for the S_{surf} (defined in eq 7):

$$S_{\text{surf}} \approx - \sum_{R_i < l_0}^{(\text{TR})} \ln(|\mathbf{R}_i^{\text{TR}}|/l_0) + \sum_{R_i < l_0}^{(\text{SQ})} \ln(|\mathbf{R}_i^{\text{SQ}}|/l_0)$$

The summation for each lattice covers all the lattice points (electrons) within a circular area of radius l_0 , the number $N = n(\pi l_0^2)$ of electrons is the same for the two lattices. The two terms each contribute a term of magnitude $\pm N \ln(l_0)$, which cancel. Rescaling ($r_i = R_i n^{1/2}$),

$$S_{\text{surf}} \approx - \sum_{r_i < l_0 \sqrt{n}}^{(\text{TR})} \ln(r_i^{\text{TR}}) + \sum_{r_i < l_0 \sqrt{n}}^{(\text{SQ})} \ln(r_i^{\text{SQ}})$$

While each sum depends on the radius $l_0 n^{1/2}$ of the circle, the difference does not. This can be seen by considering a radius r , and then increasing the radius by a small amount δr ; the number of electrons in the shell is $\delta N = n \times 2\pi r \delta r$ for either lattice, and therefore the change in each sum is equal to $\delta N \log r$, which cancel. There is thus no effect of increasing the radius $l_0 n^{1/2}$ of the circle we're summing over, i.e., S_{surf} is independent of the density n . A S_{surf} vs n plot is provided as an inset in figure 1.

-
- * Electronic address: masud@physics.rutgers.edu
† Electronic address: ipaul@physics.rutgers.edu
- ¹ E.P. Wigner, Phys. Rev. **46**, 1002 (1934)
 - ² E.Y. Andrei, *Two-Dimensional Electron Systems on Helium and other Cryogenic Substrates*, Kluwer Academic Publishers (1997)
 - ³ D.S. Fisher, B.I. Halperin, P.M. Platzman, Phys. Rev. Lett. **42**, 798 (1979)
 - ⁴ C.C. Grimes & G. Adams, Phys. Rev. Lett. **42**, 795 (1979)
 - ⁵ V.B. Shikin & P. Leiderer, Sov. Phys. JETP **54**(1), 92 (1981).
 - ⁶ P. Leiderer, article on the multi-electron dimple phenomenon, in E.Y. Andrei's compilation².
 - ⁷ P. Gor'kov & D. M. Chernikova, JETP Lett. **18**, 68 (1974), Sov. Phys. Dokl. **21**, 328 (1976).
 - ⁸ H. Ikezi, R.W. Giannetta, and P.M. Platzman, Phys. Rev. **B25**, 4488 (1982); also H. Ikezi, Phys. Rev. Lett. **42**, 1688 (1979).
 - ⁹ The polaronic state for electrons on a liquid substrate has been discussed by many authors, e.g., N. Studart & S. S. Sokolov's article in E.Y. Andrei's compilation², and references therein.
 - ¹⁰ L. Bonsall and A.A. Maradudin, Phys. Rev. **B15**, 1959 (1977).
 - ¹¹ L. Kramer, Phys. Rev. **B3**, 3821 (1971)
 - ¹² A.J. Dahm, article discussing electrons on thin helium films, in E.Y. Andrei's compilation².
 - ¹³ I. Skachko & E.Y. Andrei, private communication.
 - ¹⁴ The possibility exists that the insulating state of 2D electrons in heterojunctions may be some sort of (possibly modified) Wigner crystal state, see, e.g., S. Chakravarty *et al*, Phil. Mag. **B 79**, 859 (1999) and E. Abrahams *et al*, Rev. Mod. Phys. **73**, 251 (2001). In the Quantum Hall community, there has been discussion of Wigner crystal states interlaced between Laughlin-liquid states as a function of filling fraction, and related possibilities, see, e.g., R. Narevich *et al*, Phys. Rev. **B 64**, 245326 (2001); K. Yang, F.D.M. Haldane, & E.H. Rezayi, Phys. Rev. **B 64**, 081301 (2001); and references therein. Also, for an insulating 2D electron system under large magnetic field, attempts have been made to explain the measured AC response in terms of an assumed pinned Wigner crystal state, see R. Chitra *et al*, Phys. Rev. **B 65**, (2002), and references therein.
 - ¹⁵ J.N. Tan *et al*, Phys. Rev. Lett. **75**, 4198 (1995); A. W. Vogt, Phys. Rev. Lett. **A 49**, R657 (1994).
 - ¹⁶ R. Côté *et al*, Phys. Rev. Lett. **78**, 4825 (1997); and references therein.
 - ¹⁷ C. Timm, S.M. Girvin, and H.A. Fertig, Phys. Rev. **B 58**, 10634 (1998); S. Sankararaman & R. Shankar, cond-mat/0209160;
 - ¹⁸ M. Born and K. Huang, *Dynamical Theory of Crystal Lattices*, Oxford University Press, 1954; reprint 1988.
 - ¹⁹ A.J. Dahm *et al*, J. Low Temp. Phys. **126**, 709 (2002), quant-ph/0111029; M.I. Dykman, P.M. Platzman and P. Seddighrad, cond-mat/0209511.